Effect of Substrate Temperature on the Hydrogen Reflection at Metal Surfaces *)

Jhoelle Roche M. GUHIT, Kenta DOI and Motoi WADA

Graduate School of Science and Engineering, Doshisha University, Kyotanabe, Kyoto 610-0394, Japan

(Received 10 January 2019 / Accepted 8 April 2019)

Doppler-broadening of the Hα emission spectra from hydrogen reflected at surfaces of palladium and tungsten sheet metal surfaces held at clamp holders were presented in this study. The reflected hydrogen atoms were observed with velocity components produced by the back scatterings of H_3^+, H_2^+ and H^+ ion incident regions. Palladium exhibited higher spectrum emission intensities than tungsten for both clamp structures. Modification of the clamp structure should produce cooler surface condition due to direct contact of metal surface to the substrate holder thus having H atoms adsorbed more on the palladium sheet.

Keywords: hydrogen reflection, Doppler-broadening mechanism, palladium, tungsten

DOI: 10.1585/pfr.14.3401098

1. Introduction

Hydrogen plasma interaction on metal wall surfaces causes surface permeation or erosion and plasma impurity emission in which investigating and analyzing these phenomena are significant in the advancement of fusion research and device development. The phenomena must be studied before fusion devices will be put into operation with the long life-time. It is consequently of interest to examine and understand the underlying mechanisms of hydrogen isotope permeation and particle release during plasma-surface interactions [1, 2]. Permeation of hydrogen through metallic materials like palladium is of vital concern to control transport and mass separation of hydrogen isotopes in the system. Palladium (Pd), in comparison to tungsten (W), has a strong absorbance of hydrogen molecules and can show unique behavior in a hydrogen plasma environment due to the nature of rapid hydrogen isotope transport [3]. Thus, a comparative study in hydrogen reflection between Pd and W has been made using a small plasma exposure device [4].

The material temperature is an important parameter that determines the hydrogen transport in the bulk media, while it also affects the amount of hydrogen atoms adsorbed on the surface. Thus, the impact due to the target surface cooling for palladium and tungsten during plasma exposure in a magnetized hydrogen plasma is presented in this paper. With two different target design structures, the data on velocity distribution functions of hydrogen atoms reflected at metal surfaces will be discussed.

author's e-mail: cyjb3303@mail4.doshisha.ac.jp

*) This article is based on the presentation at the 27th International Toki Conference (ITC27) & the 13th Asia Pacific Plasma Theory Conference (APPTC2018).

2. Experimental Methods

The plasma bombardment experimental device setup is shown in Fig. 1. This apparatus irradiated palladium (Pd) and tungsten (W) metal sheets by a linear magnetized hydrogen plasma. These metal materials are 0.1 mm thick, 24 mm wide and 25 mm long in size. An 18.7 mT magnetic field is produced by three pancake coils. Each coil current input is 5 A and connected in parallel around the device to create linear magnetic-force lines that extended the electrons from the tungsten filament cathode to the target substrate holder. The embedded circuit diagram for the filament region indicates two DC power supplies, in series connection, are used to extract electrons from the filament and generate the hydrogen gas discharge. Both power supplies are maintained with discharge current of $I_2 = 1.0$ A and 70 V for both V_1 and V_2 for applied potentials. Hydrogen gas pressure is set at 1.2 Pa. These conditions generate a hydrogen cylindrical-shaped magnetized plasma with a diameter is $\Phi = 15$ mm. A viewing port of BK7 (borosilicate glass) is fitted with an ICF70 flange for the alignment of the substrate holder and hydrogen reflection measurement.

The floating potential, V_f, was approximately -8 V

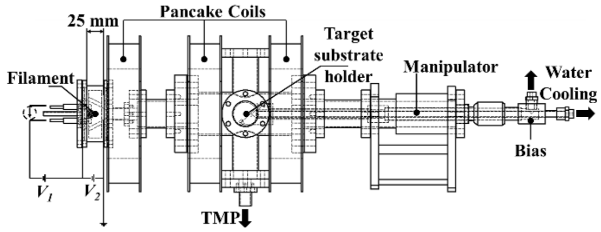

Fig. 1 Hydrogen bombardment device with embedded circuit diagram for the filament discharge region.

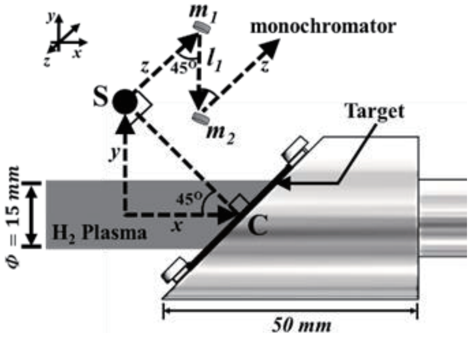

Fig. 2 Plasma diagnostic observation area from the metal sheet.

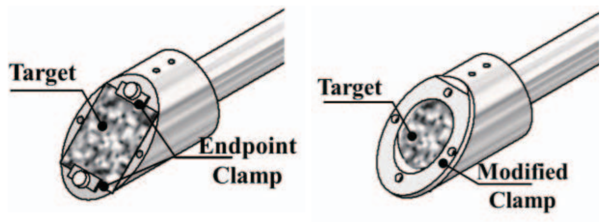

(a) (b)

Fig. 3 (a) Endpoint and (b) Modified Clamp.

and −12 V with respect to the chamber wall that was fixed at the anode potential for Pd and W, respectively. Negative bias voltages were applied to the substrate holder starting from −100 V at an increment of −100 V to −600 V maximum through a DC power supply. The −600 V is the maximum limit for the current device configuration. The molecular and atomic spectra at the vicinity of the bombarded metal sheets of Pd and W were observed through a 0.23Å wavelength resolution Czerny-turner monochromator. The wavelength used for Hα observation was set around 656.28 nm to monitor the atomic emissions. A continuously cooled CCD detector, S7034-1007S of Hamamatsu Photonics, with 60 seconds integration time recorded the output spectra.

Figure 2 illustrates the observation area for the plasma diagnostic for the hydrogen emission spectra. Ions in the hydrogen plasma, bombarded the center of the metal sheet target positioned at a 45-degree angle. The location ***C*** is denoted as the center of the metal substrate holder. This center is aligned with the epicenter of the view port through a guide laser. The substrate target holder position is adjusted in the x-axis right direction through the manipulator by 9 mm from the center, ***C***. The spot ***S***, indicated by a filled circle, is the observation of interest to detect and investigate the Doppler-broadening due to the velocity distribution of hydrogen reflection at the tungsten and palladium metal sheets. By setting the line of sight outside of the plasma column, all lines emissions from molecules directly excited by plasma electrons are excluded in the spectrum [4]. The first mirror, m_1, is perpendicular through the z-axis of the spot. It is moveable at the y-axis direction where $l_1 = 9$ mm. A second mirror, m_2, is placed below and not moveable. Both m_1 and m_2 are angled at 45 degrees. The light from the plasma is guided to the monochromator through m_1 and m_2 mirrors outside the chamber. The adjustments on the manipulator and positioning of m_1 are made to observe the emission spectra outside the plasma boundary. This mirror is set to observe perpendicularly the area of interest. The ***S*** region is perpendicular from the metal surface and approximately 12.7 mm in measurement.

An endpoint fixture structure and a ring clamp structure were utilized to hold the metal sheet target in position of the water-cooled target holder (Fig. 3 (a) and Fig. 3 (b)). In the endpoint fixture structure or the endpoint clamp, small rectangular stainless-steel washers press the metal target to the water-cooled body by the screws. The second structure of modified clamp press the peripheral part of the metal target evenly with the ring fixture to realize a better heat transfer from the thin metal target to the surface of the water-cooled target holder (Fig. 3 (b)). A continuous water flow at the backside of the holder was maintained to avoid excessive heating of the target, as temperature exceeded 1100 K during a hydrogen plasma bombardment onto the target maintained with the structure of Fig. 3 (a) [5]. Meanwhile, the surface temperature of the target mounted by the modified clamp cannot be evaluated as the temperature was below 800 K, which was the detection limit for the infrared radiation thermometer. Effect on the Doppler-broadening of the hydrogen plasma on tungsten and palladium sheet metal targets are investigated between these two target holder structures.

3. Experimental Results

Hydrogen reflection of tungsten and palladium have been compared between endpoint and modified clamp structures. The reflection characteristics were recognizable under a floating potential and increasing bias voltages with values of −100 V, −200 V, −300 V, −400 V, −500 V, and −600 V. Figures 4 (a) and 4 (b) shows the normalized intensity of the Balmer-α line spectrum emission of the S spot region of the palladium target using an endpoint clamp in linear and in semi-logarithmic scale, respectively. Figure 4 (a) illustrates an expansion of the Doppler-broadening due to the velocity distributions of hydrogen atoms excited by the collisions with H_2 molecules to the surface. Comparing the −600 V and at the floating potential, −8.76 V, the former exhibits a wider line spectrum width than the latter. This indicates that the velocity distributions, from the dissociative excitation of H_2 molecules, is prominent at increasing negative bias voltages. Figure 4 (a) also displays the blue and red wings of the Doppler shift in the negative and positive region of $\Delta\lambda$, respectively. Taking the spectra at −600 V, the blue and red wing under the endpoint clamp shows minimal difference. As the target bias was raised from −8.76 V floating

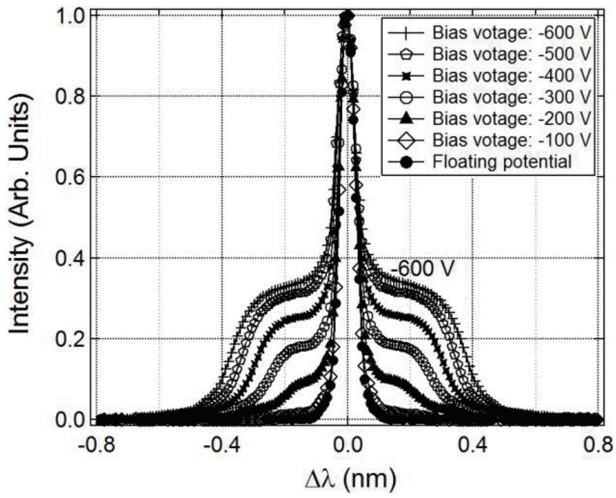

(a)

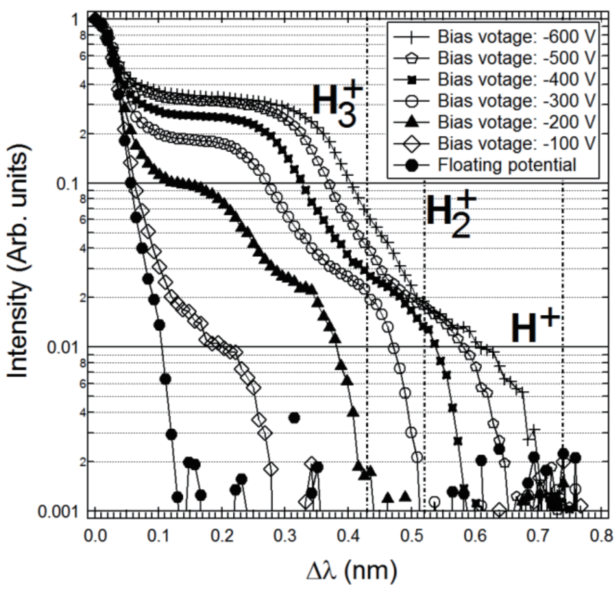

(b)

Fig. 4 Doppler-broadening spectrum, in (a) linear and (b) semi-logarithmic scale, of the magnetized hydrogen plasma on palladium target under an endpoint clamp. The spectrum broadens with increasing negative bias voltages.

potential up to −600 V, the spectrum displays enlarged red and blue wings corresponding to the incident kinetic energies of hydrogen ions. In addition, the ion species reflected are H^+, H_2^+, and H_3^+ can be observed (Fig. 4 (a)). However, to exhibit a clearer view of the reflected ions, a semi-logarithmic graph is displayed (Fig. 4 (b)). Ion species present in the plasma are H^+, H_2^+, and H_3^+ with the fraction composition changed due to particle recycling process at the target surface.

The regions of the incident ions can be separated into three according to the general equation of wavelength shift, $\Delta\lambda$, calculated by the following equation.

$$\Delta\lambda = \frac{\lambda_\alpha}{c}\sqrt{\frac{2eE_b}{M}}. \tag{1}$$

Here, λ_a is the wavelength of H_α or 656.28 nm, e is the charge of the electron, E_b is the bias voltage at −600 V, M is the mass of the ion and c is the speed of light. Equation 1 determines the regions where contributions from which ions are present. For example, at −600 V E_b, only the hydrogen atoms produced by reflection of H^+ ions at the target forms the spectrum in the wavelength from 0.52 nm to 0.74 nm. The cut-off energies of atoms formed by the reflections of H_2^+ ions, and those of H_3^+ ions determine the wavelength range from 0.43 nm to 0.52 nm as the part constituted by reflections of H^+ and H_2^+. The dissociative excitation of the background H_2 molecules produce light emission forming the sharp central peak with $\Delta\lambda < 0.5$ nm.

Figure 4 (b) shows the wavelength spectrum of light emissions from hydrogen atoms H^+, H_2^+, and H_3^+ reflections at Pd surface for the corresponding wavelength range. Intensities are normalized at the central peak. At the highest bias voltage of −600 V, the Doppler-broadening shoulder extended outward up to 0.7 nm, close to the value corresponding to 600 eV kinetic energy proton, due to excitation collisions with hydrogen molecules.

Figures 5 (a) and (b) exhibits the palladium's hydrogen emission spectrum taken with the modified clamp at normalized intensity shown in linear and semi-logarithmic scale, respectively. From floating potential to −600 V bias voltage, a widening of spectrum is seen due to prominent presence of H_2 molecules dissociative excitation at increasing negative bias voltage (Fig. 5 (a)). The blue and red wing regions of the palladium target using the modified clamp demonstrates minute difference.

From equation 1, velocity distribution regions of H_3^+, H_2^+, and H^+ are seen in Fig. 5 (b). Similar cut-off energies at $E_b = -600$ V and expansion of the Doppler-broadening shoulder up to $\Delta\lambda = 0.7$ nm is present.

Hydrogen ion reflection from tungsten and palladium metal sheets with both manifold clamps are seen in Figs. 6 (a) and (b). Velocity distributions of the ion reflection is separated by bias voltages of $E_b = -100$ V and $E_b = -600$ V. From Eq. 1, at $E_b = -100$ V, the wavelength shift for H_3^+, H_2^+, and H^+ are $|\Delta\lambda| \leq 0.17$ nm, $0.17\text{ nm} \leq |\Delta\lambda| \leq 0.21$ nm, and $|\Delta\lambda| \geq 0.30$ nm, respectively. On using either the endpoint or modified clamp, there is no remarkable change on the velocity distributions H_2^+ and H^+ regions on tungsten surface. There is minimal change to no significant change in the H_3^+ region for $E_b = -600$ V and $E_b = -100$ V, respectively, on tungsten surface when using either of the two clamps.

On the other hand, Fig. 6 (b) displays the comparison of the effect of both endpoint and modified clamps on the hydrogen reflection on the surface of the palladium metal sheet with bias voltages $E_b = -100$ V and $E_b = -600$ V. At $E_b = -100$ V, there is a prominent gap region wherein there is an observed lower emission spectrum on the endpoint clamp region relative to the modified clamp. Palladium with bias voltage $E_b = -600$ V also exhibited higher emission spectra, under the modified clamp, relative to the

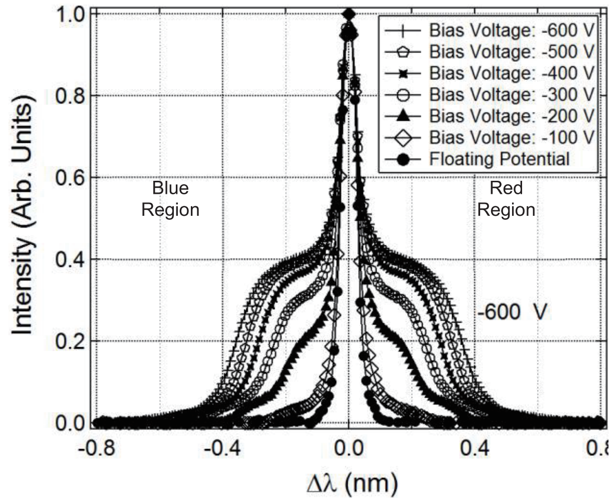

(a)

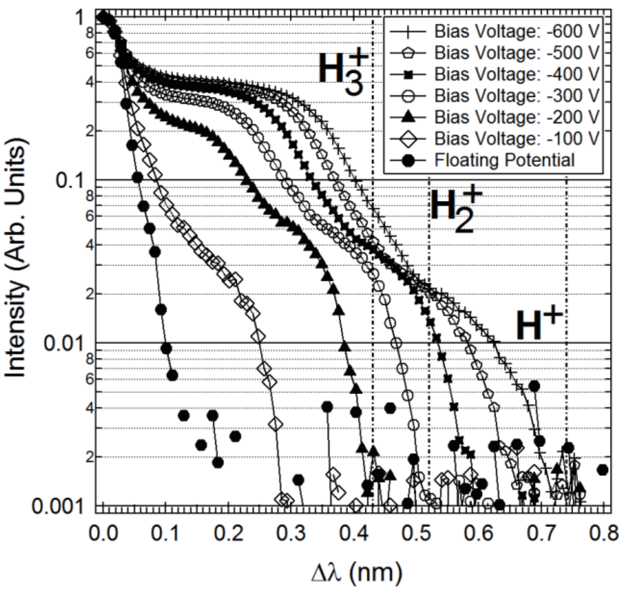

(b)

Fig. 5 Doppler-broadening spectrum, in (a) linear and (b) semi-logarithmic scale, of the magnetized hydrogen plasma on palladium target under the modified clamp. The spectrum broadens with increasing negative bias voltages.

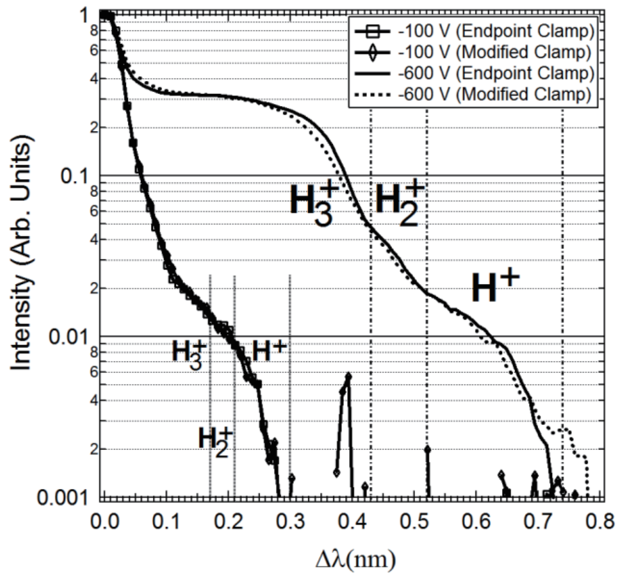

(a)

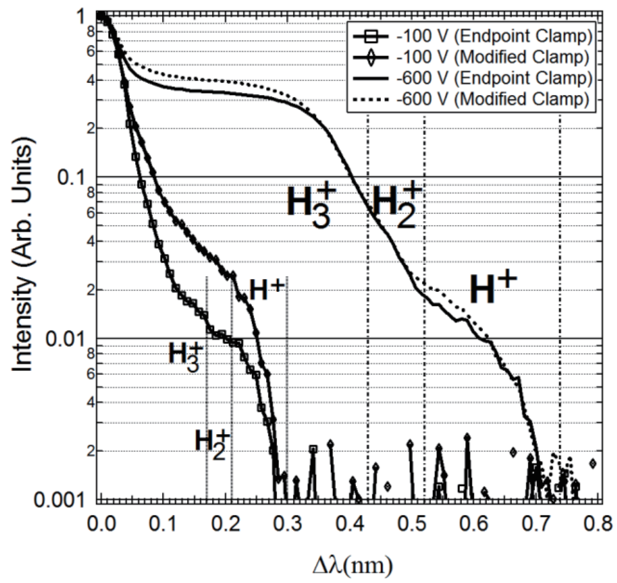

(b)

Fig. 6 Doppler-broadening spectrum (a) Tungsten and (b) Palladium in both endpoint and modified clamp. The spectral graph of -100 V and 600 V negative bias voltage are compared with each other using both clamps.

reflection distribution when endpoint clamp was used. Palladium show some enhanced signal on the H^+ and H_3^+ incident ion region when using a modified clamp. Modified clamp's impact on the emission spectra for palladium may indicate that the surface temperature on the metal sheets during bombardment also changed due to the full peripheral clamping of the second manifold. Placing a modified clamp, instead of an endpoint clamp, over the palladium metal created a direct contact with the surface backside cooling water. On the other hand, the endpoint clamp, were there is less cooling contact of the metal target, may create a mechanism where there are more adsorb molecules on the surface which may result to lesser hydrogen proton reflection. When using the infrared radiation thermometer, temperature was not completely detected for the modified clamp due to the 800 K detection limit for the infrared radiation thermometer.

Figure 7 shows the hydrogen reflection on palladium metal sheet under modified clamp in certain cases wherein there is noticeable difference in hydrogen reflection for diverse surface conditions. Conditions where compared from a spectra captured during continuous plasma process and after substrate cooling effect were applied. After substrate water cooling, higher emission spectrum relative to the continuous plasma process is observed. There is a change in spectra with regards to relative temperature and

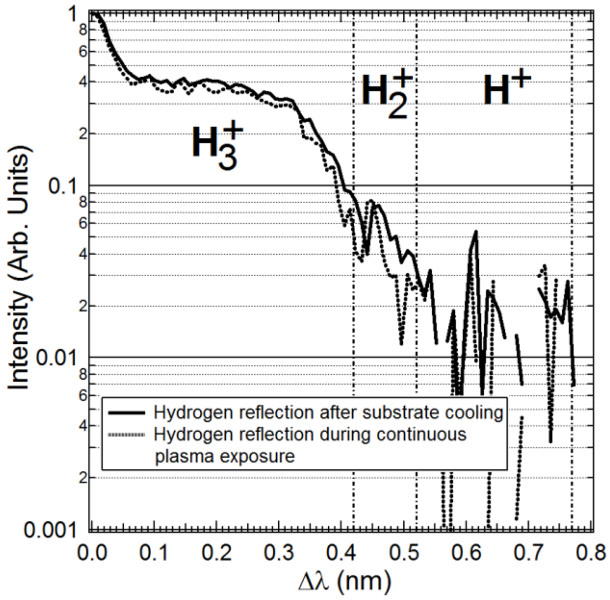

Fig. 7 Hydrogen reflection on palladium after substrate cooling and exposure to continuous plasma under modified clamp.

condition of the metal surface target.

4. Conclusions

The endpoint and modified clamp effect on the hydrogen reflection mechanism for both tungsten and palladium were discussed. Reflection characteristics were recognizable under a floating potential and at increased bias voltages applied to metal targets under endpoint and modified clamp. Blue and red wings on the spectra were also observed to be balanced on both metal targets under both manifold holders. Hydrogen reflection and ion velocity distributions on the tungsten surface have minimal difference when using either an endpoint or modified clamp. This phenomenon was observed at different bias voltages also.

Meanwhile, hydrogen velocity distributions for palladium surface showed a difference between emission spectrum for both manifolds. Modified clamp provided higher velocity distributions relative to the endpoint clamp at different bias voltages. It is suggested that better cooling was present through direct contact of the metal substrate on the substrate holder. This mechanism may provide less adsorbed hydrogen molecules and have higher Doppler-broadening distribution of emission spectra relative to using an endpoint clamp.

It is also interesting to relate results to thermocouple data diagnostic to measure the surface temperature since current setup do not contain aforementioned mechanism.

[1] G. Ramos *et al.*, J. Phys. Conf. Ser. **591**, 012031 (2015).
[2] A.P. Zakharov *et al.*, J. Nucl. Mater. **241-243**, 52 (1997).
[3] B. Sakintuna *et al.*, Int. J. Hydrog. Energy **32**, 1121 (2007).
[4] K. Doi *et al.*, IEEE Trans. Plasma Sci. **46**, 482 (2018).
[5] K. Doi *et al.*, Fusion Eng. Des. **136**, 100 (2018).